Effect of sediment pulse grain size on sediment transport rates and bed mobility in gravel bed rivers

J. G. Venditti,[1] W. E. Dietrich,[2] P. A. Nelson,[2] M. A. Wydzga,[3] J. Fadde,[4,5] and L. Sklar[4]

Received 20 June 2009; revised 13 January 2010; accepted 26 March 2010; published 25 September 2010.

[1] Sediment supply to gravel bed river channels often takes the form of episodic sediment pulses, and there is considerable interest in introducing sediment pulses in stream restorations to alter bed surface grain size distributions and bed mobility. A series of laboratory experiments was conducted in order to examine how sediment pulse grain size and volume affects the mobility of bed material in gravel bed channels. Pulses used in the experiments were composed of either the fine tail or the median of the subsurface bed material grain size distribution. Bed material refers to sediment in the channel prior to the pulse introduction exclusively. Both types of pulse were finer than the bed material surface median. Two pulse sizes were used, which were either equivalent to the volume of sediment required to cover the entire bed one median subsurface bed material grain diameter deep (full unit) or 1/4 of this volume (1/4 unit). The latter was designed to produce a transitory pulse. With the exception of the 1/4 unit coarse pulse, introduction of the sediment pulses to the channel caused dramatic increases in the bed load flux. The coarse sediment pulses fine the bed surface and coarsen the bed load. Finer pulses also fine the surface, but the bed load fines while the bed material load (that excludes pulse material) coarsens. The greatest effects on the fractional transport occurred during the full unit fine pulse where the pulse covered the greatest bed surface and effectively smoothed the bed, increasing near bed velocity and mobilizing the coarse particles. Overall, the coarse pulses were not very effective at mobilizing bed material. The large fine pulse mobilized ~35% of the bed material surface (~35% of its input weight) and was most effective at mobilizing the surface. However, the small fine pulse mobilized 50% of its input weight as it passed through the channel, making it the most efficient at mobilizing the bed material.

Citation: Venditti, J. G., W. E. Dietrich, P. A. Nelson, M. A. Wydzga, J. Fadde, and L. Sklar (2010), Effect of sediment pulse grain size on sediment transport rates and bed mobility in gravel bed rivers, *J. Geophys. Res.*, *115*, F03039, doi:10.1029/2009JF001418.

1. Introduction

[2] Sediment supply to gravel bed rivers is notoriously episodic and can often take the form of large-scale sediment pulses that can occur through anthropogenic disturbances in the watershed [e.g., *Gilbert*, 1917; *Wolman*, 1967] or by natural geomorphic processes such as landslides or debris flows from tributaries [e.g., *Roberts and Church*, 1986; *Madej and Ozaki*, 1996; *Lisle et al.*, 2001]. Ultimately, the dynamics of these episodic sediment pulses control the dynamics of sediment transport in the channel and are key to understanding longer-term dynamics and form of gravel bed channels.

[3] The dynamics of sediment pulses in gravel bed channels has received considerable attention, resulting in a wide array of field observations [see *Lisle et al.*, 2001; *Lisle*, 2008, for reviews], physical modeling efforts [*Lisle et al.*, 1997; *Cui et al.*, 2003a], and 1-D numerical models [*Cui et al.*, 2003b, 2005]. This work has largely focused on the observation and modeling of bed elevation change through time to determine if large-scale sediment pulses are dispersive or translational in nature (as hypothesized by *Gilbert* [1917] in his seminal treatise on the issue). Results suggest that bed material pulses in gravel are, in fact, largely dispersive, as opposed to translational [*Lisle et al.*, 2001] and that there is a Froude number (*Fr*) effect that controls this phenomenon [*Lisle et al.*, 1997]. Providing that there is an upstream sediment source, a bed material wave will propagate upstream if flow is supercritical ($Fr > 1$; *Fr* is defined at

[1]Department of Geography, Simon Fraser University, Burnaby, British Columbia, Canada.
[2]Department of Earth and Planetary Science, University of California, Berkeley, California, USA.
[3]Department of Earth Science, University of California-Santa Barbara, Santa Barbara, California, USA.
[4]Department of Geosciences, San Francisco State University, San Francisco, California, USA.
[5]Stillwater Sciences, Berkeley, California, USA.

0148-0227/10/2009JF001418

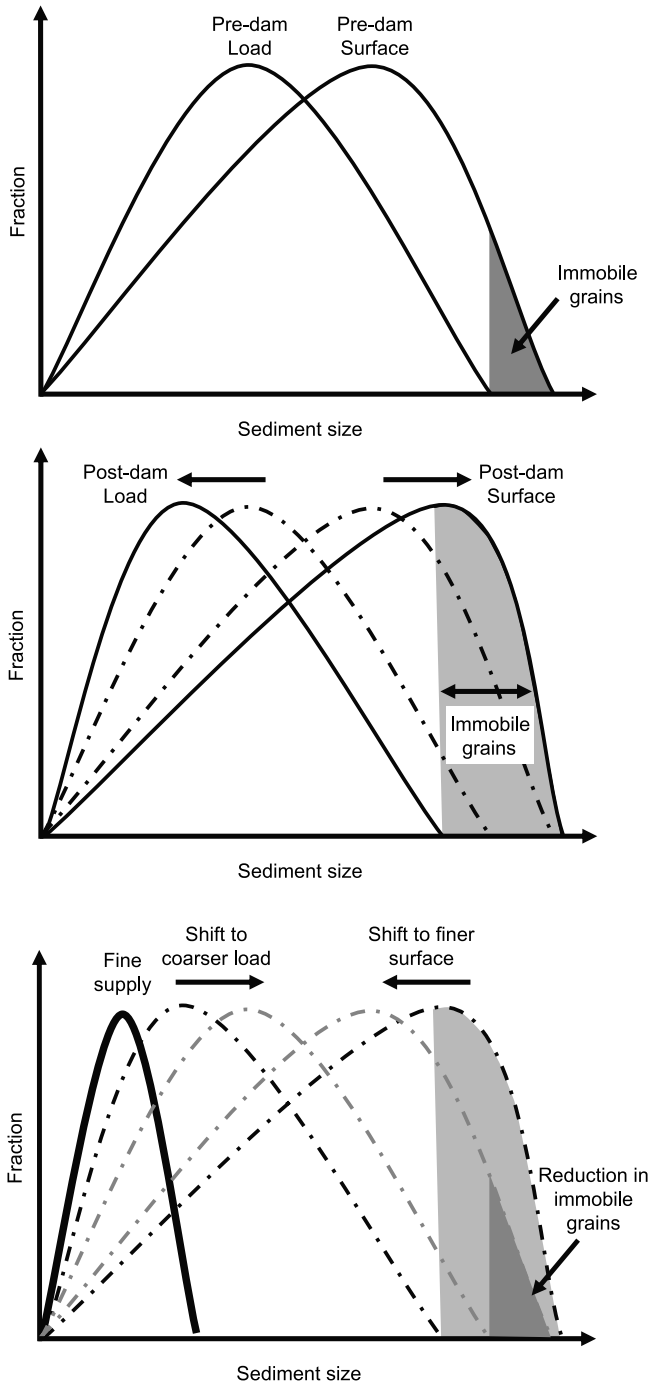

Figure 1. Shifting of surface and load grain size distributions due to sediment supply reduction and gravel augmentation. (a) Predam condition. (b) The response of the channel to a sediment supply reduction. (c) The augmentation supply distribution is hypothesized to shift size distributions in Figure 1b back to the size distributions in Figure 1a.

bankfull discharge), will disperse in place when the Froude number is transcritical ($Fr \approx 1$), and will translate downstream under subcritical flows. The dominance of dispersion is supported by the argument that flow is near a transcritical condition during flows sufficient in strength to mobilize pulse materials. Relatively little work has focused on pulse dynamics and their effects on bed mobility in channels without an upstream sediment supply. However, recent work by *Sklar et al.* [2009] suggests that while pulses often exhibit dispersive behavior, pulse grain size and volume play an important role in whether a pulse will display significant translational behavior without an upstream sediment supply. They show small-volume pulses, and pulses composed of the fine tail of the bed material grain size distributions show a greater tendency for translational behavior.

[4] The practice of gravel augmentation, the addition of sediment pulses to a river, is now common practice in rivers where dams and gravel mining have effectively eliminated sediment supply and lead to coarse, nearly immobile beds of poor habitat quality [*Harvey et al.*, 2005; *Bunte*, 2004]. The goal of these augmentations is to increase river bed mobility and fine the median bed surface to a size suitable for salmon spawning and rearing (7–47 mm) [*Kondolf and Wolman*, 1993]. The goals are strongly intertwined since sediment supply exerts a dominant control on the grain size of gravel bed surface materials [*Dietrich et al.*, 1989; *Lisle et al.*, 1993; *Nelson et al.*, 2009]. Our research was motivated by the hypothesis that, for a given river reach, there is an optimum size distribution and pulse volume to mobilize and fine the bed surface, and specifically, the addition of sufficient finer gravel may mobilize the coarse surface, fine the bed surface, and release finer subsurface material.

[5] Here we explore the effects of sediment pulses on bed mobility in channels with coarsened bed surfaces due to diminished supply (e.g., as would occur after a dam closure). To discuss the effects of sediment additions, we need to distinguish between partial, selective, and equal mobility. A universally accepted definition of these terms does not exist. Here we follow the definitions of *Parker* [2007]. Selective transport is where all sizes on the bed are found in the bed load, but the bed load size distribution is finer than the bed surface. Partial transport is where the coarse tail of the bed load size distribution is finer than that of the bed surface. Equal mobility is where the bed load size distribution and the bed surface are the same [*Parker*, 2007]. Equal mobility of the bed load with respect to the subsurface sediment (rather than the surface) can occur in the presence of a coarse surface layer [e.g., *Parker and Klingeman*, 1982].

[6] To consider the effects of sediment supply termination by dams on bed surfaces, we examine the case where the bed load size distribution is finer then the bed surface grain size distribution, and the coarse tail of the bed surface distribution is immobile (partial transport) even during annual flood events in the predam state (Figure 1a). The predam condition could also reasonably be selective transport with mobile armor [*Wilcock and DeTemple*, 2005; *Clayton and Pitlick*, 2008]. Supply reduction causes the surface to coarsen and the transported load to fine (Figure 1b). This phenomenon occurs because coarse patches on the bed expand at the expense of finer patches when the supply is reduced. As this occurs, coarse patches on the bed become immobile and transported sediment is only sourced from the fine patches [*Dietrich et al.*, 1989, 2006; *Nelson et al.*, 2009]. A much larger component of the surface size distribution will become immobile, particularly if the supply reduction is caused by a dam that reduces peak flows as part of its operations. Adding back sediment load similar to the size before the dam will coarsen the bed load and fine the

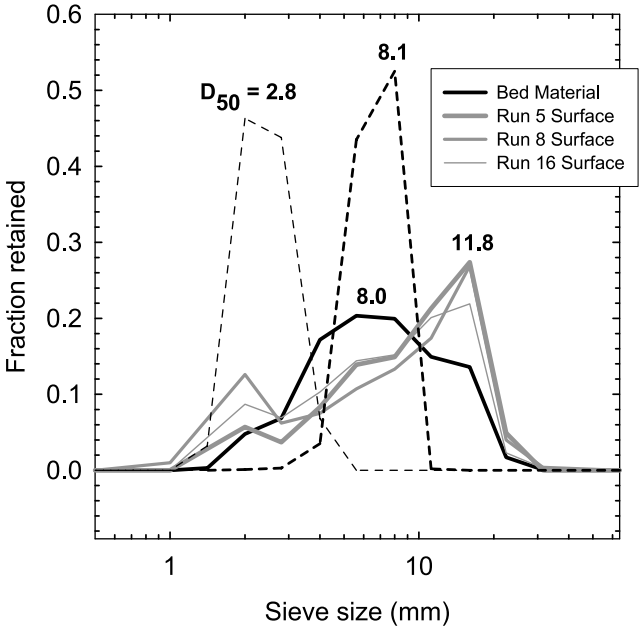

Figure 2. Sediment size distribution of the bed material, bed surface at the end of the armoring runs, and sediment pulses (thin dashed lines).

surface, reverting the channel back to the condition diagrammed in Figure 1a.

[7] We hypothesize, however, that if the added sediment is sufficiently finer than the surface, it will have a smoothing effect on the bed, accelerating near bed fluid velocities and mobilizing the bed surface rather than just covering it [*Venditti et al.*, 2010; *Dietrich et al.*, 1989; *Whiting et al.*, 1988]. In response, the load will coarsen, the surface will fine, and that portion of the surface grain size distribution that is immobile will be reduced (Figure 1c) or all grain sizes may become mobile. If this response occurs in a gravel augmentation, it has the advantage of requiring less sediment, of "unlocking" biologically unproductive armor, and, of perhaps releasing fine, permeability-reducing sediments beneath the coarse surface. In effect, we make use of the existing bed surface and subsurface materials rather than relying on burial of this resource to achieve the desired outcome. Our fundamental hypothesis is that remobilization of the bed can be accomplished without replacement of the surface by burial, and this outcome depends strongly on this size distribution and volume of the pulse.

[8] Here we test this hypothesis through a series of flume experiments in which we added pulses of various volumes and grain sizes to an immobile gravel bed in a constant subcritical flow. The role of pulse grain size, relative to the bed material, is assessed for pulses with grain sizes equivalent to the median of the bed material subsurface and the fine tail of the grain size distribution. We also consider the issue of whether the pulse magnitude and frequency is important in determining the mobilization effect.

2. Experimental Procedures

[9] Experiments were conducted in the 28 m long, 0.86 m wide, and 0.86 m deep sediment feed flume at the University of California-Berkeley. The flume bed material was composed of a unimodal gravel with a median grain size D_{50} = 8 mm and a lognormal grain size distribution truncated at 2 and 32 mm (Figure 2). We intentionally avoided adding sand to our bed material and sediment supply mixtures so we could focus on gravel interaction effects. This also avoids some potential problems with grain Reynolds scaling between field and laboratory conditions. Aspects of the experiments presented here are also presented in the work of *Sklar et al.* [2009] in a discussion of pulse translation and dispersion without an upstream sediment supply.

[10] In reporting our experiments, we use the term bed material to refer to the initial bed stock used in our experiments. This sediment formed the subsurface in the flume. The term bed load is used to describe all materials being transported in the channel and may include both the bed material and any pulse material that was introduced. Similarly, the bed surface is composed of the bed material and may include pulse material. The term bed material load is used to refer to material in transport that is sourced from the bed material and excludes pulse material.

2.1. Prototype and Scaling

[11] The experimental conditions are Froude modeled after a generic prototype of gravel bed rivers downstream of dams in the Central Valley of California. A review of unpublished data suggests that it is reasonable to assume the following prototype channel characteristics: (1) the median bed surface grain size $D_{50\text{-surf}}$ is between 64 and 128 mm with a distribution that can extend as high as 256 mm; (2) channels are heavily armored in so far as the subsurface materials are much finer than the surface; (3) channel slopes are $\sim 0.5 \times 10^{-3}$; (4) flows are subcritical, fully turbulent, hydraulically rough; (5) there is little or no sediment supply near the dam site; and (6) current bankfull flows cause strong selective or partial mobility only. Flow depths in this type of channel would be on the order of 1–2 m according to the modified Chezy equation (Parker e-book, 2009; 1-D sediment transport morphodynamics with applications to rivers and turbidity currents, e-book, 2009, available at http://vtchl.uiuc.edu/people/parkerg/morphodynamics_e-book.htm). We have further assumed that at bankfull flows the Shields number for the bed surface is just below the threshold of motion. The Shields number is defined as

$$\tau_* \equiv \frac{\tau_b}{(\rho_s - \rho_w) g D} \tag{1}$$

where τ_b is the shear stress at the bed, D is the diameter of a particle and is usually taken as the surface median size for heterogeneous bed particles, ρ_s and ρ_w are the densities of the sediment and fluid, respectively, and g is gravitational acceleration. Values of $\tau_* < 0.045$ are widely accepted as characterizing conditions below the entrainment threshold for a gravel mixture [*Miller et al.*, 1977; *Yalin and Karahan*, 1979].

[12] Using this prototype and a scaling ratio of either 1:4 or 1:8, an experimental model is realized with flow depth d = 22 mm and $D_{50\text{-surf}}$ = 16 mm (Table 1). As in the prototype, flows in the model are fully turbulent, hydraulically rough, and lower regime in terms of the Froude

Table 1. Scale-up of Model Parameters to Field Prototype Scale

Parameter	Model	Prototype (1:4)	Prototype (1:8)
S	~0.0045	~0.0045	~0.0045
d (m)	0.22	0.88	1.76
$D_{50\text{-surf}}$ (mm)	16[a]	64	128
τ_*	0.038	0.038	0.038
$Re \times 10^6$	0.24	1.9	5.5
$Re_g \times 10^5$	0.12	0.95	2.7
Fr	0.75	0.75	0.75

[a]Based on an area-by-weight sample of the surface material. $Fr = \bar{U}/(gd)^{0.5}$ is the Froude number ($\bar{U}$ is the mean velocity, g is gravitational acceleration, and d is the flow depth). $Re = d\bar{U}/\nu$ is the Reynolds number (ν is the kinematic viscosity), and $Re_g = Du_*/\nu$ is the grain Reynolds number ($u_* \equiv (\tau/\rho)^{0.5}$ is the shear velocity, $\tau = \rho gSd$, τ is the boundary shear stress, S is the channel slope, and ρ_w is the water density). $\tau_* = \tau/[gD(\rho_s - \rho_w)]$ is the Shields number (D is a grain size taken as the median here and ρ_s is the sediment density).

number (Table 1). A fundamental difference between the model and the prototype is the width-to-depth ratio w/d. In open channels with a mobile bed and banks, w/d typically exceeds 20, while in the model, $w/d = 4$. This flow geometry was chosen to suppress the development of lateral topography and allows us to focus on grain-to-grain interactions. As such, our flume should be thought of as slice through a much wider channel rather than a full-width channel.

2.2. Pulse Size and Addition

[13] Experiments proceeded by establishing an equilibrium grade and transport rate by feeding sediment with the same size distribution as the flume bed material at ~40 kg/h, until the sediment began exiting the channel at roughly the same rate. Then, in order to model a dam closure scenario, we continued the flow but eliminated the sediment supply for a period of at least 24 h. Ultimately, eliminating the sediment supply coarsened the bed significantly by eliminating finer patches, reduced the channel slope by ~10% of its original value, and dramatically reduced the sediment transport rate. We conducted three of these feed reduction experiments (runs 5, 8, and 16). The responses of the channel to these conditions are discussed in detail by *Nelson et al.* [2009] and are summarized in Table 2.

[14] Following the supply elimination, a series of narrowly graded painted gravel pulses (Figure 2) were added over a period of 25–100 min at a rate that was ~4× the bed load rate observed prior to terminating the sediment supply (~160 kg/h). A total of seven experimental runs were conducted with the same channel slope, discharge, and bed sediments. The runs differed in the mass of the gravel pulse added to the channel, pulse grain size, and the frequency of pulse additions (Table 3). Pulses were composed of either 3 or 8 mm gravel material (Figure 2). The 3 mm gravel pulses were composed of the material that makes up the fine tail of the bed material grain size distribution originally placed in the flume before the experiments while the coarser 8 mm gravel pulse composed the core of that distribution. Both size distributions were finer than the bed surface median size. When all the relevant dimensions are scaled up to prototype scale, the additions that we discuss here are equivalent to adding 12 mm particles to bed with $D_{50\text{-surf}}$ = 64 mm at a 1:4 scaling or 24 mm particles to a bed with $D_{50\text{-surf}}$ = 128 mm 1:8 scaling (Table 1).

[15] Three types of pulses were used in the experiments: (1) single addition pulses with a mass equivalent to the volume that would cover the bed one bed material median grain size ($D_{50\text{-BM}}$) deep over 1/4 of the flume (1/4 unit pulses; runs 6, 9, and 23), (2) single addition pulses that could cover the bed one $D_{50\text{-BM}}$ deep over the length of the flume (full unit pulses; runs 7 and 10), and (3) multiple additions of 1/4 unit pulses added to the flume in sequence with a short intervening period (runs 12 and 21). The volumetric calculations assume the loosest possible sediment packing and a sediment density of 2650 kg/m^3. The total added in the multiple pulse run is the same as a full unit pulse.

[16] Runs 23 and 21 were repeats of runs 6 and 12, respectively. These were conducted to verify results and so we could take additional measurements that were not obtained during the earlier run. The difference between the paired runs were subtle, so we discuss them interchangeably depending on which one provided the measurements required to make a specific argument.

2.3. Measurements

[17] We monitored the pulse movement in the flume, its effect on bed and water surface topography, as well as bed load transport, bed load grain size, and bed surface grain size. The bed surface and water surface elevation were monitored using an ultrasonic water level sensor (manufactured by Massa Products Corp.) and an acoustic echo sounder (manufactured by the National Center for Earth Surface Dynamics). At the beginning and end of each run and when possible during a run, the water surface and bed surface elevation were measured at 5 mm intervals along five longitudinal profiles spaced at 218 mm in the cross-stream direction with the center transect located along the center of the flume. The channel slopes reported herein are based on an average of the three center profiles, omitting the profiles 50 mm from both sidewalls, which did not reflect the active portion of the bed.

Table 2. Changes in Channel Slope, Bed Surface Grain Size, and Bed Material Transport After Eliminating the Sediment Supply

		S (mm/m)			$D_{50\text{-surf}}$[a] (mm)			Q_s (kg/h)		
Run	t (h)	Init	End	Δ	Init	End	Δ	Init	End	Δ
5	23	4.8	4.3	−0.5	15.5 (8.8)	16.4 (11.9)	0.7 (3.1)	49.0	6.0	−88%
8	82	4.3[b] (4.7)	4.3	*0.0 (−0.4)	n/m	16.6 (10.9)	n/a	37.8	1.1	−97%
16	62	4.0	4.4	−0.4	n/m	14.8 (9.9)	n/a	39.2	2.2	−94%

[a]Weight-by-area sample. Value in brackets has been converted to a weight-by-volume sample using the *Kellerhals and Bray* [1971] conversion. n/m, not measured. See *Nelson et al.* [2009] for further discussion of these data.
[b]Slope peaked at 4.7×10^{-3} m/m and began declining before the feed was cut off due to a transient scour hole at the head of the flume.

Table 3. Pulse Characteristics and Hydraulic Conditions for Gravel Sediment Pulses in the Order in Which They Were Conducted

	Pulse Characteristics			Hydraulic Conditions						
Run	Pulse Type	Pulse D_{50} (mm)	Mass (kg)	d (mm)	S ($\times 10^{-3}$)	U (m/s)	Fr	$D_{50\text{-surf}}$[a] (mm)	$D_{90\text{-surf}}$[a] (mm)	τ^*[b]
5end	Initial condition	n/a	n/a	228[c]	4.33	1.04	0.70	16.4 (11.9)	22.8 (21.0)	0.035
6	Small coarse pulse	8	50.3[d]	230[c]	4.19	1.04	0.69	14.2 (9.5)	22.3 (20.1)	0.039
7	Large coarse pulse	8	267.3	234[c]	4.08	1.06	0.71	15.3 (9.4)	24.4 (20.7)	0.034
8end	Initial condition	n/a	n/a	229	4.27	1.05	0.70	16.6 (10.9)	22.8 (20.9)	0.034
9	Small fine pulse	3	66.8	231	4.20	1.03	0.69	16.0 (9.2)	23.3 (20.5)	0.035
10	Large fine pulse	3	267.3	242	4.13	0.99	0.64	16.3 (10.0)	23.8 (20.8)	0.035
12	Multiple fine pulses (labled a, b, c, d in order)	3	4 x 66.8	235	4.02	0.99	0.64	16.4 (9.4)	22.4 (20.5)	0.034
16end	Initial condition	n/a	n/a	239	4.04	1.00	0.65	14.8 (9.9)	21.7 (20.0)	0.037
21	Multiple fine pulses (labled a, b, c, d in order)[e]	3	4 x 66.8	244	4.00	0.98	0.63	16.5 (10.7)	24.8 (21.1)	0.034
23	Small coarse pulse[e]	8	66.8	244	3.68	0.98	0.63	15.0 (10.0)	22.7 (20.5)	0.034

[a]Weight-by-area physical sample of bed surface. Value in brackets has been converted to a weight-by-volume sample using the *Kellerhals and Bray* [1971] conversion.
[b]Sidewall corrected using the relation reported by *Williams* [1970].
[c]Flow depth measurements from the end of run 5, run 6, and run 9 contained systematic errors, so depth was estimated using the Manning-Strickler equation: $d = [(k_s^{1/3} q_w^2)/(\alpha^2 gS)]^{3/10}$, where $k_s = 2D_{50}$, q_w is the specific water discharge, $\alpha = 8$ [*Parker*, 2009].
[d]Feed rate = 30.8 kg/h.
[e]Repeats of earlier runs.

[18] Bed load was monitored using a continuous weighing mechanism that captured all sediment exiting the flume in a drum suspended in the end tank from a load cell that recorded the weight of material at 1 s intervals. Minor contamination of the signal persists when the weighing drum was nearly empty and able to move easily due to turbulence in the end tank for long periods of time. With ~1 kg of sediment in the collection drum, this contamination disappears. Hence, we elected to use 60 s sampling intervals. Sections of the record were also removed when the drum was nearly empty and transport rates were low.

[19] At each stage of the experiment, subsamples of the material collected by the weighing mechanism were dried and sieved for grain size analysis. The amount of material sieved was selected such that the largest particle (32 mm) was <0.1% of the total sample weight [see *Church et al.*, 1987] and, in most cases, there was enough material to meet this criterion. We sampled the bed surface material at the beginning and end of the run by spray painting a 0.25 m^2 at x = 10, 15, 20, and 25 m in the center of the flume and removing the painted particles, which were also sieved. In order to augment the physical bed surface samples, we also obtained photos of the bed surface any time the bed load was collected from the weighing mechanism and analyzed the photos obtained at ~2 m increments along the bed using a grid-by-number technique in a GIS software package that is similar to a Wolman count [*Bunte and Abt*, 2001]. The sampling grid laid over the images covered 52% of the flume width.

[20] The variety of methods used to obtain grain size distributions can produce slightly different results for the same sampled material. Bed load is a weight-by-volume sample that should be roughly equivalent to the grid-by-number technique [*Church et al.*, 1987], but the weight-by-area surface samples need to be converted to a weight-by-volume sample for direct comparison of grain sizes using the *Kellerhals and Bray* [1971] conversion. No systematic sampling of the subsurface material was undertaken. As such, we have assumed the subsurface composition is equivalent to the size distribution originally placed in the flume.

3. Pulse Morphodynamics and Effects on Bed Load Transport Rates

[21] Once introduced into the channel, the pulse material quickly begins to move downstream, reaching the end of the channel after ~40 min for the fine pulses and ~2 h for the coarse pulses. Pulses tend to show a mix of translational and dispersive behaviors, but 1/4 unit, fine pulses showed a greater tendency for translation [*Sklar et al.*, 2009].

[22] The passage of each pulse varied with pulse size distribution and volume. Figure 3 shows a fine sediment pulse (run 21b) as it migrated beneath a stationary deployment of the water surface and bed surface profiler. There are at least two distinct wave scales that are present including the broad topographic signature of the pulse and smaller-scale low-amplitude, nearly symmetric migrating waves that make up the broad topographic wave. At their maximum thickness, the low-amplitude bed waves have a cross-stream extent ~3/4 width, but between each bed wave, the bed material is exposed. The large coarse pulse (run 7) had roughly the same form. The small coarse pulses (runs 6 and 23) had no identifiable topographic effect, but discrete mobile patches still formed and migrated downstream periodically partially burying and exposing the original bed material. By 5–10 m downstream, however, these patches had dispersed.

[23] Figure 4 shows bed load transport exiting the channel Q_s for each of the single-pulse experiments. The response in Q_s varies depending on both the grain size and volume of the pulse. Fine pulses display a well-defined peak and a prolonged period after the peak over which Q_s remains higher than the background prepulse transport rate. Peak sediment transport rates for fine pulses are larger than the

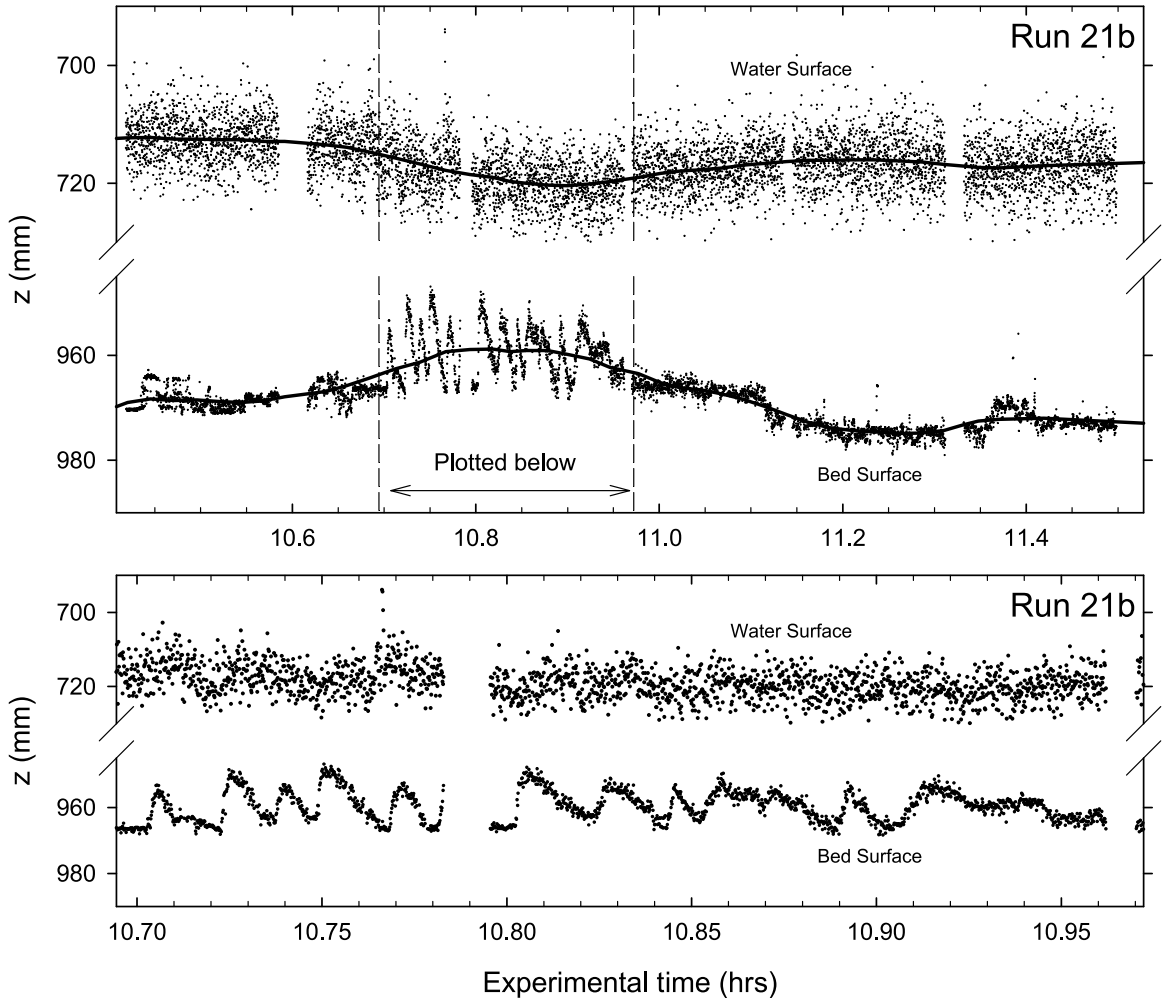

Figure 3. Sediment pulse wave scales observed in the center of the channel during run 21b 20 m downstream of the flume entrance and 15 m downstream from the feed point. Gaps in the time series are periods when no measurements were obtained.

input rates Q_{in} and instantaneous (60 s average) Q_s can be as high as $2 \times Q_{in}$ when individual low-amplitude waves are exiting the channel. The duration of the Q_s peak is roughly equivalent to the duration of the feed for the fine pulses and represents the period when the main topographic signature of the pulse is exiting the channel. After the main body of the fine pulses has left the channel, Q_s remained at ~30 kg/h and then declined back to the prepulse rate (1.3 kg/h for run 9 and 2.4 kg/h for run 10) over the next 10–12 h. The shape of the declining sediment flux curve is remarkably similar for both the large and small fine sediment pulses. This slow decline arises in part from the progressive removal of pulse sediment from temporary storage in the bed surface. The fine pulses also alter the surface armor, releasing subsurface sediment [*Venditti et al.*, 2010], and the duration of declining sediment flux partly represents the period over which the bed is rearmored.

[24] Sediment flux associated with the coarse pulses responds differently from the fine pulses in many respects. In contrast to the fine pulses, peak Q_s values for the large coarse pulse do not exceed the Q_{in} and the period of declining sediment transport rates is not as well defined as for the fine pulses. The small coarse pulse, while making a distinct topographic rise initially, completely disperses by the time it reaches the end of the flume and causes no flux variation there.

4. Bed Load and Bed Surface Grain Size Responses to Sediment Pulses

[25] Evidence of bed mobilization in the bed load was traced by quantifying that fraction of the total bed load flux, which was painted (introduced with the pulse), and that fraction that was unpainted (hence, derived from the bed). Here we use "pulse material" to refer to the original painted sediment introduced at the upstream end of the flume. Bed material load refers to that part of the bed load that is unpainted (and hence, not part of the introduced sediment).

4.1. Evolution of Bed Load Grain Size

[26] In each run, the fraction of the bed load composed of pulse material jumps to a maximum value when the peak flux arrives and then the proportion of pulse material in the bed load progressively declines (Figure 5). With the

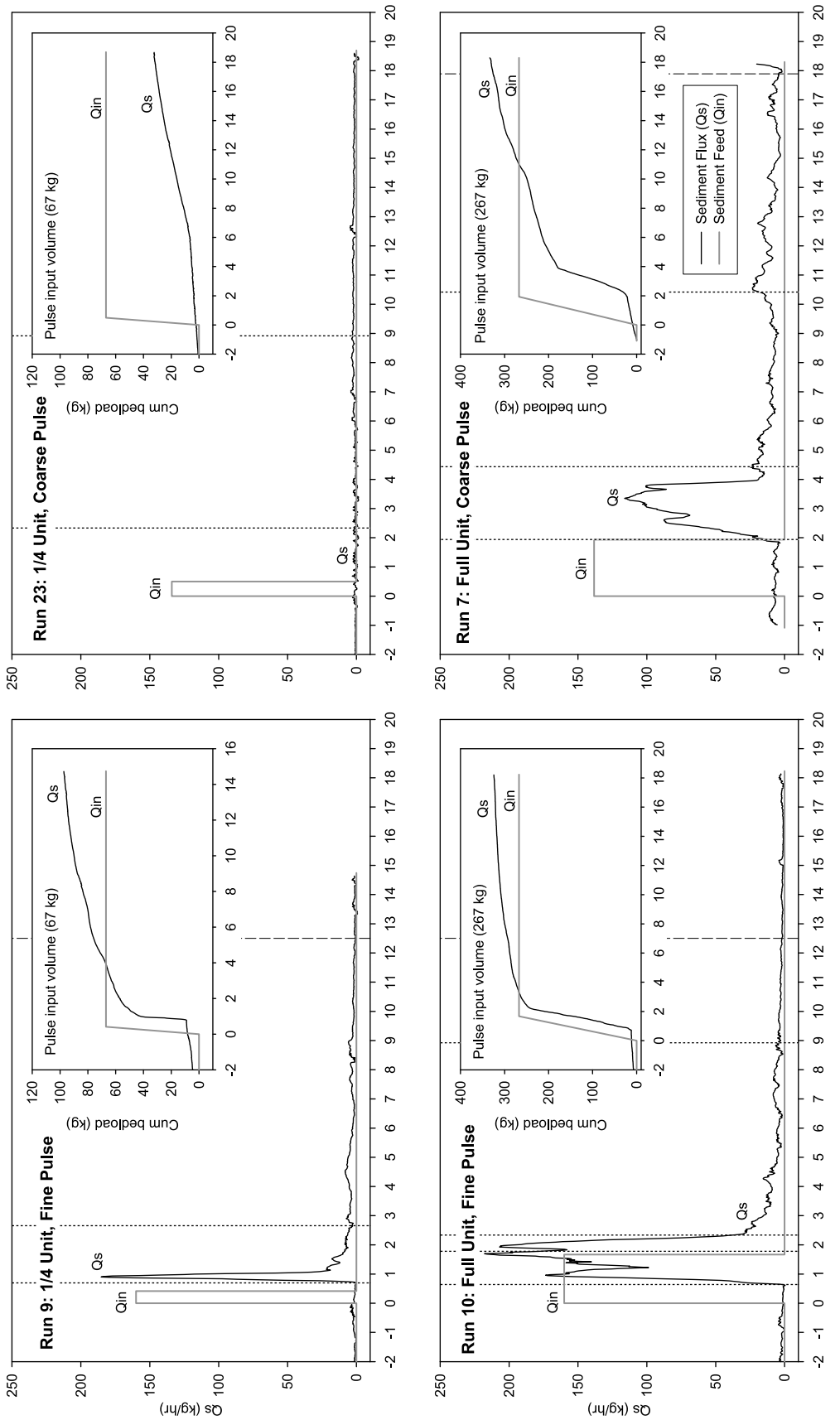

Figure 4. Measured bed load transport at the end of the flume during the single-pulse experiments (runs 23, 7, 9, and 10). Sediment flux curves are 5 min running averages. Vertical short-dash lines represent periods when the flume was stopped to obtain the bed load materials from the collection mechanism and for photos of the bed surface grains size distributions. The vertical long-dash lines indicate when the effects of the pulse on transport rates has ended, which is designated as the time when the transport rate systematically declines to the prepulse rate.

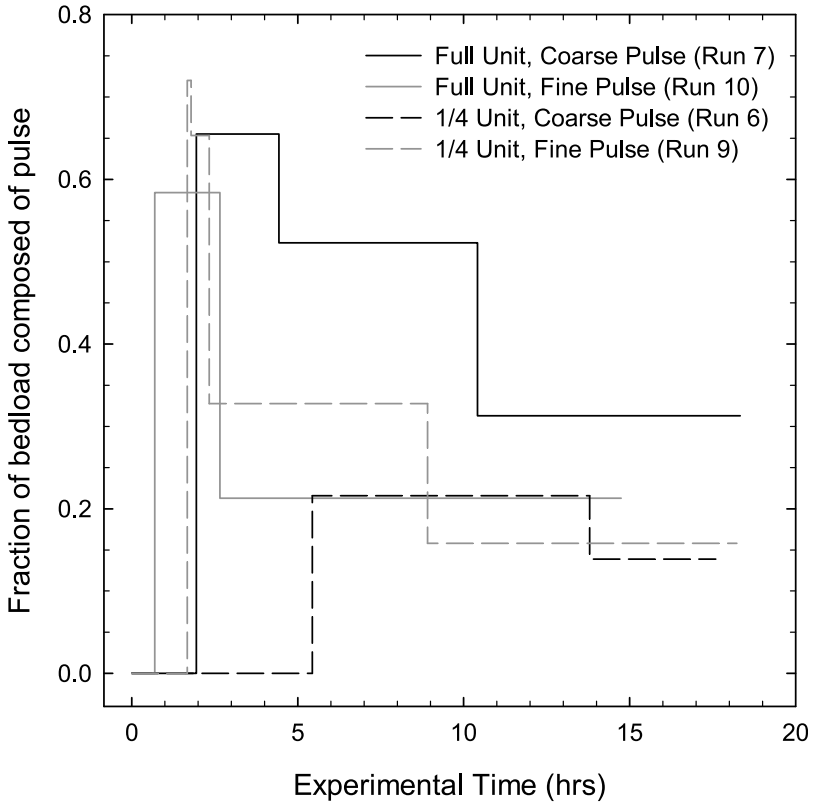

Figure 5. Fraction of the bed load composed of sediment pulse material. The left corner of the square curve represents a sample. The flat portion of the square curve extends over the time period for which that sampling point was used in calculations of the bed material load.

exception of the 1/4 unit coarse pulse, the peak fraction of pulse material in the bed load exceeds 50%. The coarser pulses have longer lasting effects on the composition of the bed load, indicating a longer residence time for the pulse particles in the flume. For the 1/4 unit coarse pulse (run 6, which is similar to run 23 in Figure 4), the pulse only arrived at the downstream end of the flume about 5 h after its introduction, and correspondingly, only 22% of the arriving sediment was pulse material. None of our experiments lasted until the fraction of the bed load composed of the pulse material returned to zero.

[27] In response to the sediment pulse, the bed load grain size distribution shifts from the prepulse condition to a size distribution dominated by the pulse material, but the magnitude of the change is mediated by the initial transport regime in the experiments. This is demonstrated in Figure 6, which shows the median bed load ($D_{50\text{-BL}}$), median bed material load ($D_{50\text{-BML}}$), and bed surface ($D_{50\text{-surf}}$) grain sizes as they evolve in the experiments. The prepulse sediment transport regime varied somewhat in our experiments because some runs began with a zero feed bed condition while others used a bed inherited from sediment pulse runs (see Table 3 for the sequence of runs). Figure 7 shows the grain size distributions at the beginning of all our pulse runs (Figures 7b and 7c) and for the end of all the zero-feed runs for comparison (Figure 7a). For the zero-feed runs, bed load was finer than the surface, but with all sizes from the bed present (selective transport). The size distribution of the bed load is similar, however, to the subsurface material (approaching equal mobility with regard to the subsurface), suggesting that even after extended periods of no feed, the channel surface and shear stress adjustments were still causing net removal of the underlying bed material. Figure 7b reveals that runs 6, 7, and 9 started with initial conditions characteristic of the end of the no-feed runs and hence are similar to Figure 7a. In contrast, the beginning of runs 10, 12, 21, and 23 had bed load size distributions that were much finer than both the surface and subsurface size distributions, but with all sizes from the bed present (strong selective transport) (Figure 7c). These runs were all preceded by fine pulse runs that disturbed the surface armor releasing some subsurface material [*Venditti et al.*, 2010] providing a fine sediment supply that was small enough to not affect mobility in the channel but still significant enough to skew the grain size distribution at low transport rates.

[28] In spite of the differences in the initial conditions, the changes in bed load grain size upon arrival of sediment pulse at the flume exit show similar patterns. Fine pulses cause a temporary decline in the bed load $D_{50\text{-BL}}$ to ~3mm while the coarse pulses cause a temporary increase in the bed load $D_{50\text{-BL}}$ to ~8mm (Figure 6). As the pulse material is exhausted from the bed surface, the bed load $D_{50\text{-BL}}$ recovers to its initial condition. Over some period longer than our experiments, the bed load would coarsen until it resembles the no-feed bed load condition.

4.2. Evolution of Bed Surface Grain Size

[29] The bed surface temporarily fines in response to the pulse for coarse and fine sediment pulses (both of which are considerably finer than the bed surface). Figure 6 displays

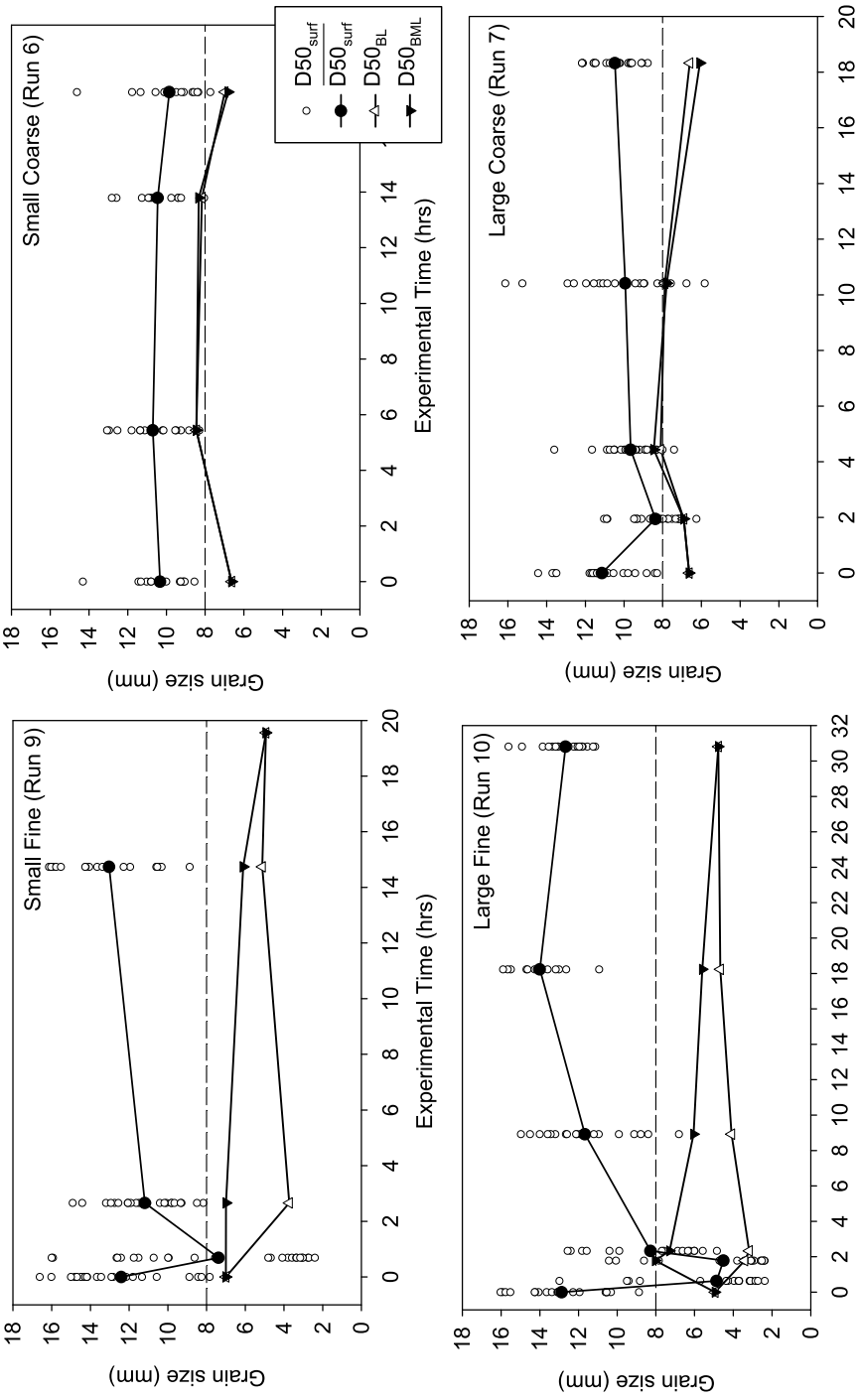

Figure 6. Median bed load ($D_{50\text{-BL}}$), bed material load ($D_{50\text{-BML}}$), and bed surface ($D_{50\text{-surf}}$) grain size time series. Open circles represent different locations along the flume and closed circles are their average at a particular time. $D_{50\text{-BL}}$ and $D_{50\text{-BML}}$ are identical at the start of all runs and are nearly identical throughout run 6 and run 7. The horizontal dashed line represents the bed material (subsurface) D_{50}.

the bed surface grain size distributions obtained from photos taken at ~2 m increments along the flume between 5 and 27 m. The first sample is before the pulse is introduced to the channel. The second measurement is after the pulse has traveled nearly the full length of the flume, but before the pulse has begun to exit the channel. Subsequent measurements demonstrate the depletion of pulse sediment from the surface. The mean values of $D_{50\text{-surf}}$ show consistent trends in fining due to the pulse material addition and then a subsequent return to prepulse size distribution. The fining associated with the fine pulses is of greater magnitude and of shorter duration than the coarser pulses (Figure 6). The coarse 1/4 unit pulse (run 6) does not significantly affect $D_{50\text{-surf}}$, because the pulse particles tend to disperse into the surface.

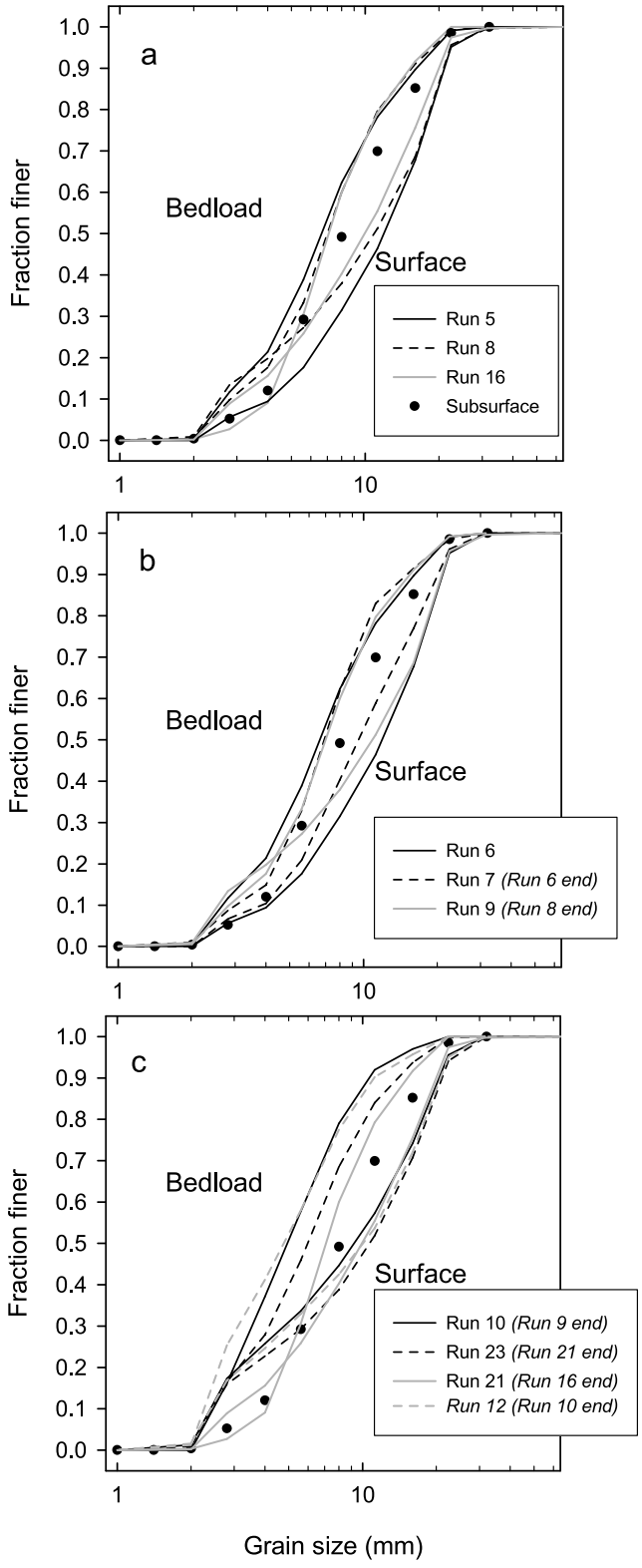

Figure 7. Initial bed load and bed surface grain size distributions for (a) the end of the zero-feed runs, (b) pulse runs that began with a near-equal mobility condition, and (c) pulse runs that began with a strong selective mobility condition. Bed surface size distributions generally plot to the right of the subsurface size distribution (dots) and the corresponding bed load size distribution plots to the left. Surface size distributions were from area-by-weight samples converted to volume by weight distributions using the *Kellerhals and Bray* [1971] method.

[30] There is significant variation in $D_{50\text{-surf}}$, but there is some structure to the variation. This structure is revealed by examination of the downstream variation in $D_{50\text{-surf}}$. Figure 8 plots $D_{50\text{-surf}}$ against distance along the flume for the 1/4 unit fine pulse (run 9) and highlights patterns observed during all the runs except the coarse 1/4 unit pulses. There is a downstream fining trend in the flume before the sediment pulse is introduced and after the sediment pulse has exited the flume. Once the pulse has been introduced to the channel, $D_{50\text{-surf}}$ varies between 2 and 5mm where the pulse covers the bed (at 42 min and between 15 and 24 m downstream in Figure 8) and the original bed surface is exposed upstream and downstream of the pulse.

5. Fractional Bed Material Transport

[31] To test the mobilization effect of the pulse addition, we tracked the grain size distribution of the bed material load (unpainted) component of the bed load captured at the end of the flume in association with pulse events. Figure 6 plots the $D_{50\text{-BML}}$ through time and Figure 9 plots the fraction f_i of the bed material load composed of various grain sizes as a function of time in the experiment. The first value at zero time in Figure 9 is before the pulse reached the end of the flume and represents the prepulse condition. The grain size distribution has been binned into five categories: 1–2, 2–4, 4–8, 8–16, and 16–32 mm for display purposes. Because the grain size distribution of material in the flume was initially truncated at 2 and 32 mm, there is no material >32 mm and only a small fraction of the bed material load is in the size range 1–2 mm. Figures 6 and 9 reveal that the fine and coarse pulses affect the bed material fractions in transport in different ways.

5.1. Bed Material Fractions in Transport During Fine Pulses

[32] The bed material transport for the 1/4 unit fine pulse (run 9) remains unchanged as the pulse arrives at the end of the flume. Then there is a gradual fining of $D_{50\text{-BML}}$ from 7 mm during the pulse to 5 mm at the end of the run (Figure 6). This results from an increase in the fraction of the bed material load finer than 4 mm at the expense of

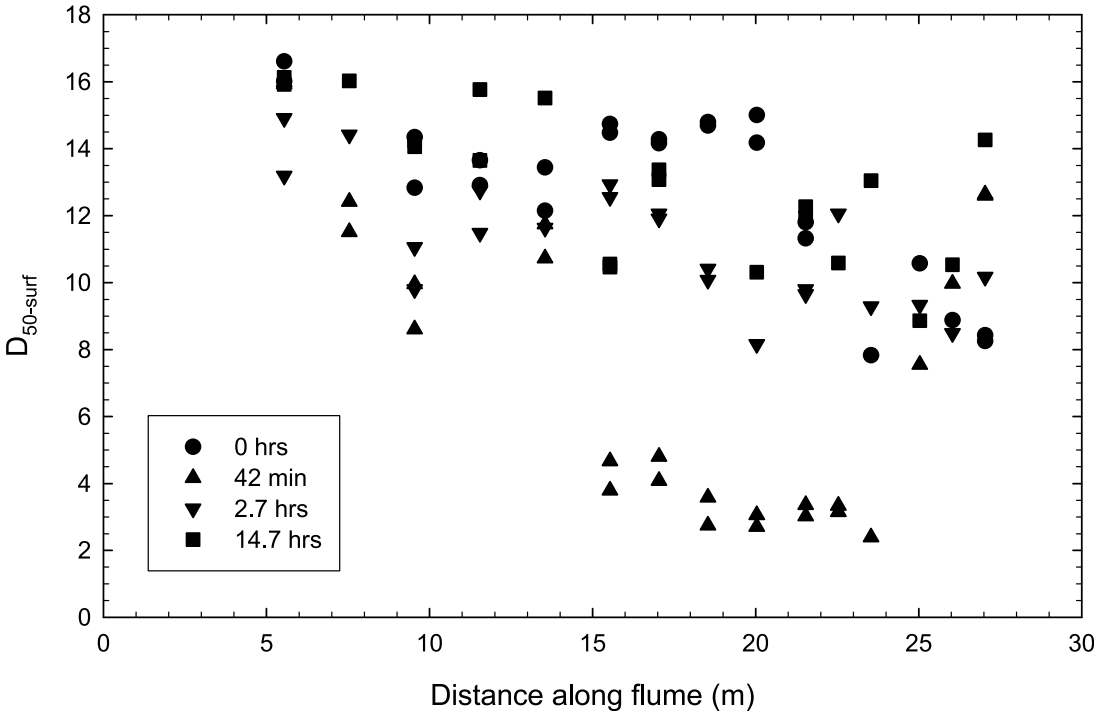

Figure 8. Downstream change in median bed surface grain size ($D_{50\text{-surf}}$) measured from photos during the 1/4 unit fine pulse run (run 9). Most photos were analyzed twice by independent analysts, and both points are shown for comparison.

material coarser than 16 mm (Figure 9). The large fine pulse (run 10) caused the bed material load exiting the flume to initially coarsen (Figure 6). Notably the 8–16 and 16–32 mm size classes represent a significantly larger fraction of the load at the pulse peak, leading to an increase in the median grain size of this load (Figure 6). After the peak the bed material load progressively fined (Figure 6) and returned to prepulse distributions (Figure 9). After ~30 h of the run, the nonpulse bed load flux has returned to the prepulse condition.

5.2. Bed Material Fractions in Transport During Coarse Pulses

[33] The coarse pulses interacted differently with the bed material in many respects. The effects of the coarse pulses are more subtle than for the fine pulses. For the 1/4 unit pulse (run 6), ~5 h after the pulse has been introduced to the channel, there is a subtle coarsening of the bed material load such that $D_{50\text{-BML}} = 8$ mm (Figure 6). This occurs due to an increase in bed material coarser than 8 mm in the load at the expense of material finer than 4 mm (Figure 9). The bed material load then coarsens back to the prepulse condition (Figure 6). A nearly identical pattern can be observed for the full unit pulse (run 10) where there is a nominal coarsening of the bed material load from a prepulse condition where $D_{50\text{-BML}} = 6.5$ mm to $D_{50\text{-BML}} = 8.5$ mm during the pulse (Figure 6). This is followed by a gradual fining of the bed load back to the prepulse condition.

5.3. Fractional Transport Rates

[34] The ultimate impact of sediment pulse grain size on bed material transport can be further understood by examining the fractional bed material transport rates. We focus on the full unit coarse and fine pulses because they have the most extensive data. In order to calculate the bed material transport rate Q_{BM} at any stage in our experiments, we begin by calculating the total sediment flux rate Q_s between the various sampling intervals and subtracting out the pulse material flux rate Q_{pulse}. The remaining bed material flux is composed of gravel that would have exited the flume whether a pulse was input or not and material that was mobilized by interactions between the bed and pulse materials. We cannot separate the mobilized bed material flux rate $Q_{BM\text{-}mob}$ from the background bed material flux rate $Q_{BM\text{-}bg}$ by observation (as we could with the painted sediment), but we can estimate $Q_{BM\text{-}bg}$ as the prepulse transport rate. This allows us to calculate $Q_{BM\text{-}mob} = Q_{BM} - Q_{BM\text{-}bg}$, which is the mobilization rate of bed material. We can also calculate the fractional bed material transport rate Q_{BMi} $Q_{BM} \cdot f_i$ and the fractional mobilization rate $Q_{BM\text{-}mobi} = Q_{BM\text{-}mob} \cdot f_i$ (where f_i denotes the fraction of size class i in the bed material load).

[35] Figure 10 shows Q_{BMi} and $Q_{BM\text{-}mobi}$ binned into the same five categories used above: 1–2, 2–4, 4–8, 8–16, and 16–32mm. Both the fine and coarse sediment pulses cause a spike in Q_{BMi} and $Q_{BM\text{-}mobi}$ across all grain sizes. The largest increases are observed in the 4–8 and 8–16 mm size classes because these are the sizes in greatest abundance in the flume. After the peak, the fractional bed material transport rates gradually return to their background rates (~10 h after the pulses reach the end of flume). Normalizing $Q_{BM\text{-}mobi}$ by the fraction of each grain size in the bed produces a result similar to that shown in Figure 10 but eliminates the spike in $Q_{BM\text{-}mobi}$ across all grain sizes for the large coarse pulse run (run 7).

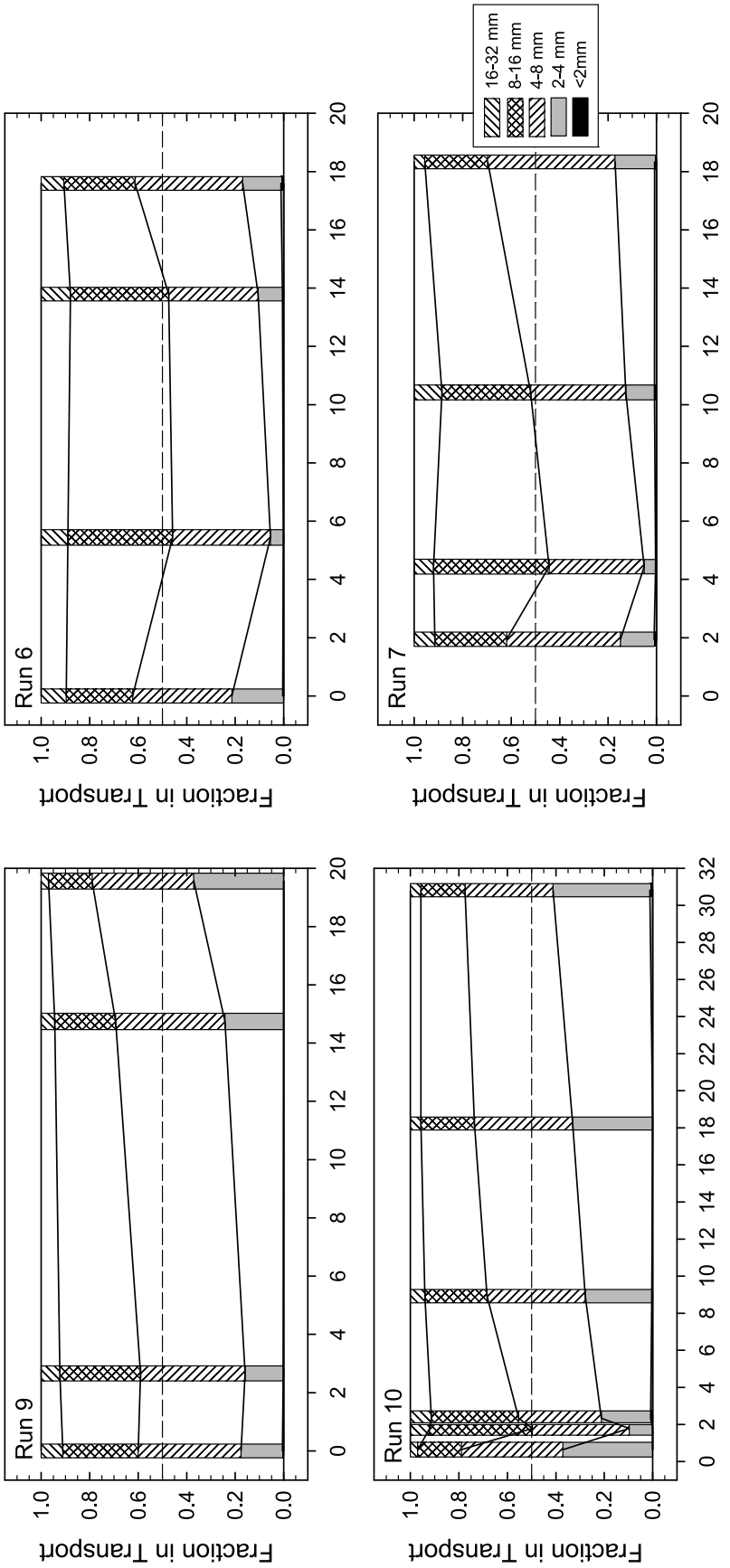

Figure 9. Fraction of bed material grain size distribution in transport for the 1/4 unit fine pulse (run 9), the full unit fine pulse (run 10), the 1/4 unit coarse pulse (run 6), and the full unit coarse pulse (run 7).

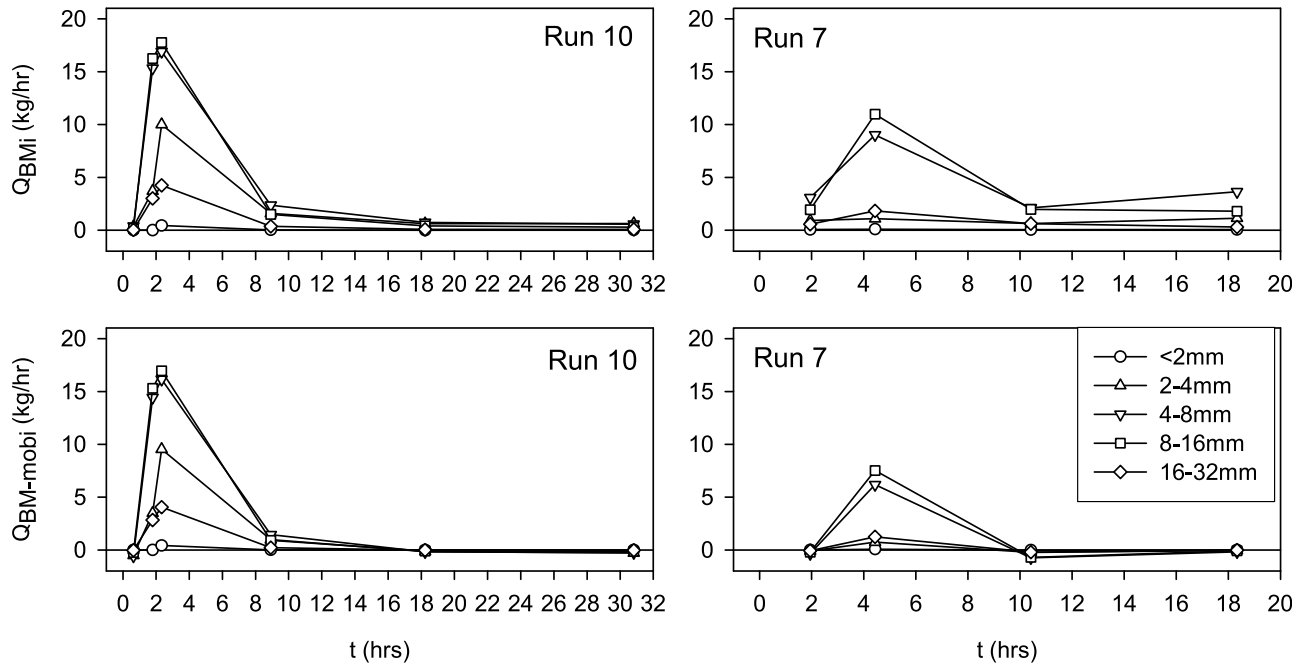

Figure 10. Fractional transport rates of the bed material (Q_{BMi}) and bed material mobilization rates ($Q_{BM\text{-}mobi}$) for the large fine pulse (run 10) and the large coarse pulse (run 7).

[36] Figure 10 shows two other important responses. First, the magnitude of increase in fractional transport rates is smaller for the coarse pulse than for the fine pulse. This suggests that the bed material mobilization rate declines as pulse grain size increases for the same pulse volume. Second, late in the fine pulse runs, when the effect of the sediment pulse has ended, Q_s drops slightly below $Q_{BM\text{-}bg}$ (the initial transport rate) such that $Q_{BM\text{-}mobi}$ is negative. This probably occurs because our $Q_{BM\text{-}bg}$ estimate is not perfect. However, during the coarse pulse runs, negative values occur in the 4–8 and 8–16 mm size classes before the end of the run and recover to near-zero values at the end of the runs. This suggests that the coarse pulse material is suppressing bed material mobilization by replacing the background transport (i.e., pulse material is being transported instead of bed material because there is more of it available on the bed).

6. Bed Material Sediment Budget

6.1. Single-Pulse Experiments

[37] The increase in fractional bed material transport rates noted above indicate that both fine and coarse pulses interact with the bed material producing a mobilization effect that influences the load and size distribution of the pulses exiting the channel. Here we quantify the interaction between pulse and bed material by calculating the mass of mobilized material by each sediment pulse using a sediment budget.

[38] The total amount of sediment that exited the channel is

$$M_{tot-out} = M_{pulse\text{-}out} + M_{BM\text{-}out} = \left(M_{pulse\text{-}in} + M_{BM\text{-}in}\right) - \left(dM_{pulse\text{-}store} + dM_{BM\text{-}store}\right), \quad (2)$$

where $M_{pulse\text{-}out}$ is the mass of the sediment pulse material that exited the channel, $M_{BM\text{-}out}$ is the bed material that exited the channel, $M_{pulse\text{-}in}$ is the pulse input mass, and $M_{BM\text{-}in}$ is the input bed material mass, which is always zero in our experiments because there was no bed material feed. The change in the mass of pulse sediment stored in the channel bed $M_{pulse\text{-}store}$ is always positive, and the change in the mass of bed material in the channel $M_{BM\text{-}store}$ is always negative in our experiments. The values of $M_{pulse\text{-}out}$ and $M_{BM\text{-}out}$ can be measured because the sediment pulses were painted. The mass of the bed material exiting the channel is further subdivided such that

$$M_{BM\text{-}out} = M_{BM\text{-}bg} + M_{BM\text{-}mob}, \quad (3)$$

where $M_{BM\text{-}bg}$ is the background bed material output mass and $M_{BM\text{-}mob}$ is the mass of mobilized bed material that exits the flume. The value of $M_{BM\text{-}bg}$ is estimated as prepulse transport rate multiplied by experimental run time. The mass of sediment mobilized by the sediment pulse is

$$M_{BM\text{-}mob} = M_{tot\text{-}out} - M_{BM\text{-}bg} - M_{pulse\text{-}out}. \quad (4)$$

The calculations are performed using observations from when the pulse was introduced to the channel to when the postpulse Q_s dropped to the prepulse transport rate (Q_{bg}).

[39] During the small coarse pulse (run 23), 73% of the pulse went into storage in the channel and the net mobilization of bed material was negligible (0.4 kg), meaning the estimated value of $M_{BM\text{-}bg} \approx M_{BM\text{-}out}$ (Figure 11). For the larger coarse pulse (run 7), 33% of the pulse went into storage and 24.1 kg of material was mobilized by the pulse (Figure 11). The fine pulses had a greater net mobilization effect per unit mass of pulse input and the storage of the small fine and large fine pulses was similar to the large

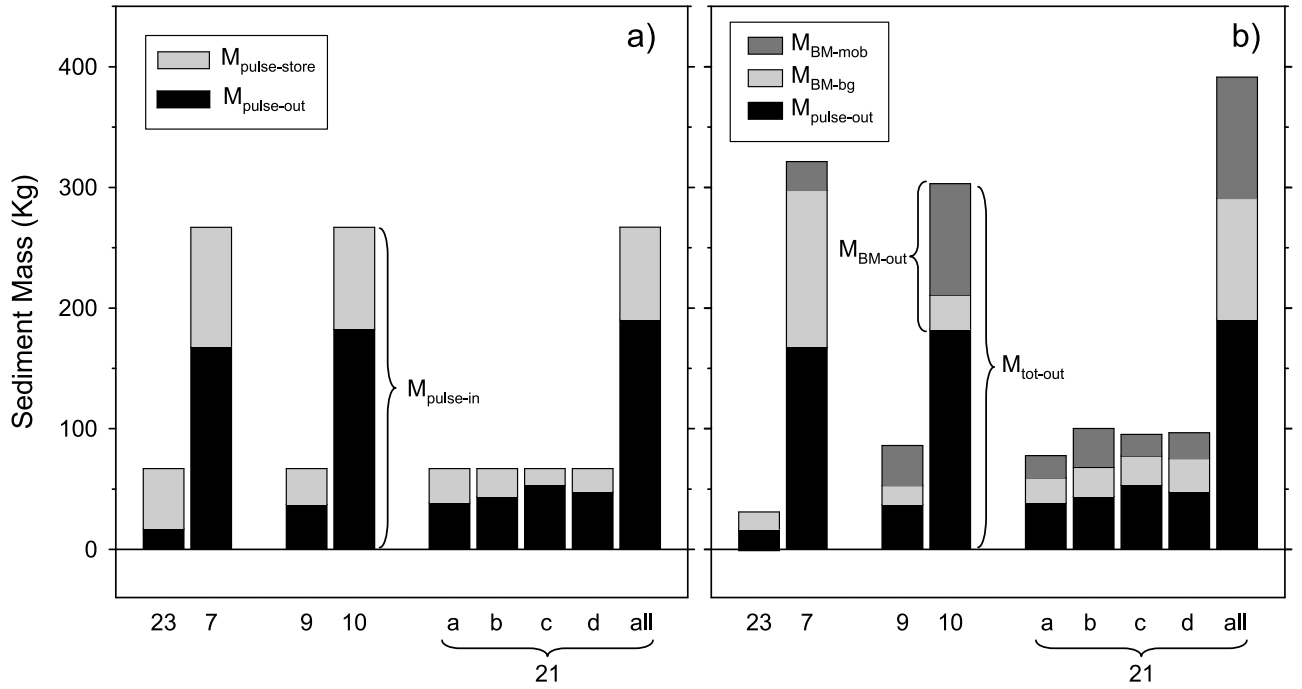

Figure 11. Mass balance for the sediment pulse and components of the total sediment flux. (a) Pulse input mass $M_{pulse-in}$ subdivided into the mass of the sediment pulse material that exited the channel $M_{pulse-out}$ and the mass of pulse sediment that was stored in the channel bed $M_{pulse-store}$. (b) Total sediment flux $M_{tot-out}$ subdivided into $M_{pulse-out}$, background bed material output mass M_{BM-bg}, and the mobilized bed material mass M_{BM-mob}. The sum of these two latter components is the total mass of bed material output M_{BM-out}.

coarse pulse. For the small fine pulse (run 9), 44% went into storage and 33.2 kg of material was mobilized (Figure 11). For the large fine pulse (run 10), 31% went into storage and 90.7 kg of bed material was mobilized (Figure 11).

[40] A measure of the effectiveness of mobilization is the ratio of M_{BM-mob} to the mass of sediment mobilization required to entrain the entire bed one D_{50-BM} deep (M_{surf}). This indicates how much of the surface layer can be mobilized for a given input of sediment. Another metric is the efficiency of a mass of sediment at mobilizing bed material $M_{BM-mob}/M_{pulse-in}$ (these two metrics are equivalent for the cases of the large pulse additions because the pulse size was prescribed to be equivalent to the mobilization of the entire bed surface 267 kg). The results (Table 4) indicate that the large fine pulse mobilized ~34% of the bed material surface (~34% of its input weight) and was most effective at mobilizing the surface. However, the small fine pulse mobilized 50% of its input weight as it passed through the channel, making it the most efficient at mobilizing the bed material. In contrast, the coarse pulses were not very effective or efficient at mobilizing the surface (Table 4).

6.2. Multiple Pulse Experiments

[41] The observations that the large fine pulse mobilized the greatest mass of bed surface material and that the small pulse was more efficient than the large pulse motivated two further experiments (runs 12 and 21) where we introduced 4 to 1/4 unit fine pulses in succession to determine if this pulse series was more efficient than adding a single full unit fine pulse. Runs 12 and 21 were identical, but we monitored different aspects of the experiments. During Run 12, we focused on obtaining a detailed time series of bed material load grain size changes, which required stopping flow and draining the flume. During run 21, we ran a more continuous experiment in which the flume was only stopped 4 times (after each pulse passage), and we monitored adjustments in the flow structure that are reported in *Venditti et al.* [2010]. Figures 12 and 13 present the resultant bed load transport output from run 21 and the grain size distributions for run 12, respectively.

[42] Bed load transport rates respond to the introduction of each 1/4 unit pulse as in the small fine pulse run (run 9). Sediment flux increases ~40 min after the pulse was fed into

Table 4. Pulse Effectiveness at Mobilizing the Surface M_{BM-mob}/M_{surf} and Pulse Efficiency $M_{BM-mob}/M_{pulse-in}$

Run		M_{BM-mob}/M_{surf} (%)	$M_{BM-mob}/M_{pulse-in}$ (%)
23	Small coarse	0.1	0.5
7	Large coarse	9.0	9.0
9	Small fine	12.4	49.6
10	Large fine	34.0	34.0
21	Small fine 1	6.9	27.4
	Small fine 2	12.1	48.4
	Small fine 3	6.7	26.8
	Small fine 4	8.1	32.1
	Average	8.4	33.7
	Total[a]	37.6	37.6

[a]The total for run 21 includes 8.3 h of the run not included in any of the individual pulses.

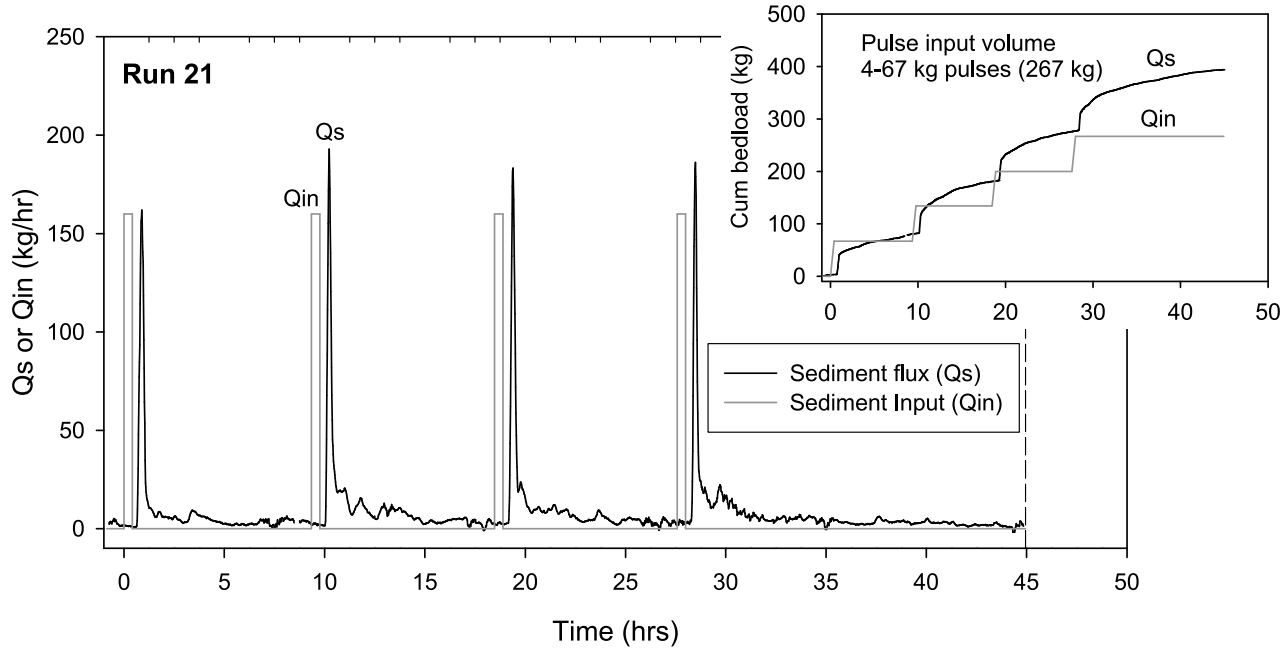

Figure 12. Measured bed load transport during the one of the multiple fine pulse experiments (run 21). The vertical dashed line indicates when the effects of the pulse on transport rates have ended, which is designated as the time when the transport rate systematically declined to the prepulse rate.

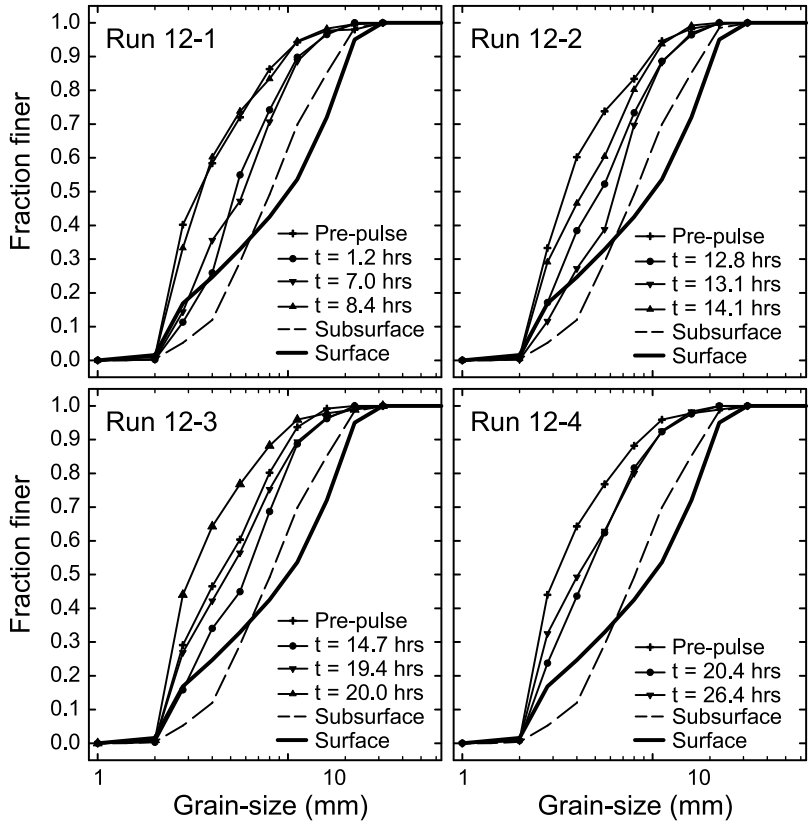

Figure 13. Bed material load grain size distributions for material exiting the channel during one of the multiple pulse experiment (run 12). The prepulse condition for 12-2, 12-3, and 12-4 is the transport condition inherited from the previous pulse. Note that there are only two samples taken during run 21-4. The final sample that for other pulses showed recovery to the prepulse condition was not taken.

the channel. The pulses exit the flume at rates larger than they were input and, after the main body of the pulse exits the channel, there is an extended period over which bed load transport rates trend slowly toward the background rate (Figure 12). In an attempt to generate a cumulative effect of the pulses, new 1/4 unit pulses were introduced to the channel before Q_s dropped to Q_{bg}, when we observed all migrating sediment patches to have left the channel. Bed material load grain size also responds to each 1/4 unit pulse in the same fashion as the single fine pulse runs, coarsening significantly and then progressively fining (Figure 13) as the effects of the pulse are diminished and the bed begins to rearmor.

[43] The masses of pulse material that exited the channel and went into storage for each subpulse, as well as the mobilized mass of bed material, were similar to the single small fine pulse run (run 9) (Figures 11). For the four 1/4 unit pulses, the pulse storage in the channel varied between 20% and 43% of $M_{pulse\text{-}in}$ (Figure 11). The calculated $M_{BM\text{-}mob}$ varies between 17.9 and 32.4 kg per individual pulse, which is less than observed $M_{BM\text{-}mob}$ during the single small fine pulse run (run 9). This occurs because we designed our experiment to produce a cumulative effect of the pulses, so the bed was not allowed to equilibrate back to the $Q_s \approx Q_{bg}$ condition, except after the last pulse when the experiment was extended for 8.3 h after all migrating sediment patches exited the flume (any additional mobilization that happened during this period is not included in the per pulse totals but is included in the final run 21 total). Our attempt to produce this cumulative effect shortened the time over which mobilization can occur after each 1/4 unit pulse, relative to the single small fine pulse.

[44] There is some pattern in the variability of $M_{pulse\text{-}out}$, $M_{pulse\text{-}store}$, and $M_{BM\text{-}mob}$ during the multiple pulse experiments. The mass of each pulse going into storage increases from the first to third pulse and then declines for the fourth pulse (Figure 11a). There is also a significant increase in $M_{BM\text{-}mob}$ for the second pulse. Values of $M_{BM\text{-}mob}$ are similar for the first, third, and fourth pulses (Figure 11b). This suggests that a single 1/4 unit pulse may be insufficient to saturate the bed material surface and that the maximum mobilization occurs after that the surface is saturated with fine particles. The pattern also suggests that the amount of mobilization declines for subsequent pulses after the maximum mobilization.

[45] The integrated effect of the multiple pulses is 9.8 kg more material was mobilized than during the full unit fine pulse experiment (run 10). This gives a 3.6% increase in the effectiveness and efficiency of the pulse (Table 4) relative to the full unit fine pulse (run 10). It is not clear that this difference is larger than the natural variability we would observe if we ran many replicates of the full unit fine pulse runs. Nevertheless, the increase in mobilization from the first to second pulses suggests multiple pulses may enhance mobility relative to a single small pulse.

7. Discussion

7.1. Effect of Pulse Grain Size on Pulse Bed Material Interaction

[46] At the outset of our experiments, we hypothesized that a sediment pulse composed of the subsurface median would coarsen the bed load and fine the surface. Our coarse sediment pulse results support this hypothesis. The ~8 mm large coarse pulse, which was finer than the bed surface, fined the surface which increased the transport rates and coarsened the bed load, which includes both pulse material and the bed material present in the channel prior to the pulse introduction. Bed material load, which excludes the pulse material, also coarsens (Figure 6). The smaller coarse sediment pulse also coarsened the bed load and bed material load, but it dispersed and did not impact the bed surface grain size (Figure 6).

[47] We further hypothesized that adding a sediment pulse much finer than the surface will coarsen the bed load, fine the surface, and that the portion of the surface grain size distribution that is immobile will be reduced. Although we did not have an immobile size fraction in our experiments, our fine sediment pulse results appear to support this hypothesis. The ~3 mm pulses fine the bed surface dramatically, increasing total bed load and bed material load. Because our fine pulses are much finer than the bed load grain size at the beginning of the each run, the bed load fines. However, if the bed material load is much finer than the bed surface and subsurface size distributions (a strongly selective transport regime), a fine sediment pulse causes a shift to a near-equal mobility condition (where bed load median size is within ~1mm of the subsurface median size) relative to the subsurface as happens during the large fine sediment pulse (Figure 6).

[48] We also hypothesized that the grain size of the sediment pulse controls the degree of the interaction between the pulse and bed material because finer pulses should have a smoothing effect on the bed, accelerating near bed fluid velocities and mobilizing the bed surface rather than just covering it [*Venditti et al.*, 2010; *Dietrich et al.*, 1989; *Whiting et al.*, 1988]. Our results also seem to support this hypothesis because the fundamental interaction of the pulse with the bed material appears to be controlled by different processes for our coarse and fine pulses. All the pulses cause a near-equal mobility bed material transport regime relative to the subsurface. This happens regardless of whether the bed load was finer than the subsurface or equivalent to the subsurface size distribution prior to the pulses. Yet the fine pulses alter the armor such that the fractional transport of the coarse tail of the size distribution is increased.

[49] In our experiments, we also found that the load fined after a fine pulse has passed through the channel and stays fine (see runs 9 and 10; Figure 6) even though the pulse material had largely been exhausted from the bed surface. This could happen through a decline in the shear stress over the experiment or a fining of the surface and exposure of subsurface material. Boundary shear stress did not decline in our experiments, suggesting that fining of the bed surface has occurred by exposure of the subsurface material. Examination of the mean surface grain size (Figure 6) does not reveal a change in the bed surface texture from the beginning to the end of the runs, but the surface grain size distribution does change from unimodal to bimodal distribution with significant amounts of fine material on the surface (see below). The effects of coarse pulses on surface armor are more moderate, and subsurface material is not exposed for long periods of time after pulse passage.

7.2. Can Sediment Pulses Eliminate or Reduce Surface Armor?

[50] The issue of whether adding sediment pulses can reduce the degree of surface armor can only be fully understood by examining changes in bed surface grain size. *Sklar et al.* [2009] provide analysis of median bed surface grain size evolution for the single-pulse experiments we present herein. They demonstrate that $D_{50\text{-surf}}$ is ~12 mm prior to the pulses in all experiments. As the pulses pass through the channel, $D_{50\text{-surf}}$ drops to the pulse grain size (8 mm for coarse pulse or 3 mm for fine pulse) and that $D_{50\text{-surf}}$ coarsens back to the prepulse state over the course of the experiments. The results of *Sklar et al.* [2009] suggest the pulses have a temporary effect on the bed material surface armor. Further examination of the grain size distributions reveal that, while this is true, patterns in the median grain size do not reflect changes in the surface grain size distribution.

[51] Figure 14 provides a summary of changes in the bed surface that occurred in response to coarse and fine pulses at the same location 15 m downstream of the pulse input site. During the feed portion of the initial condition run (run 5) for the coarse pulse run (run 7), $D_{50\text{-surf}}$ is 10.4 mm and eliminating the feed provides a moderate coarsening to where $D_{50\text{-surf}}$ = 11.6 mm. Addition of the 8 mm coarse pulse fines the bed to ~8.5 mm, and by the end of the experiment, the bed surface size distribution is similar to the bed without a sediment feed. During the feed portion of the initial condition run (run 8) for the small fine pulse (run 9), $D_{50\text{-surf}}$ = 9.7 mm and eliminating the feed provides a significant coarsening to where $D_{50\text{-surf}}$ = 14.2 mm. Introduction of the pulse fines the surface so $D_{50\text{-surf}}$ = 3 mm and $D_{50\text{-surf}}$ coarsens to 10.3 mm at the end of the run. However, the surface grain size distribution is bimodal (Figure 14, bottom right). This is partly because of pulse grains in storage on the surface, but there is finer bed material exposed here as well, which leads to the transport regime where the bed load size distribution is much finer than the surface and subsurface (strong selective transport).

[52] These data show that sediment pulses can reduce the degree of surface armoring, but the fining of $D_{50\text{-surf}}$ is temporary, which is particularly true for coarse pulses. Fine pulses have a large magnitude fining effect that is shorter-lived than for the coarser pulses in terms of the median grain size, but there is a shift to a bimodal surface grain size distribution and fining of the bed load that persists for longer periods of time.

7.3. Application to Stream Restoration or Renaturalization

[53] Our results suggest that sediment pulses finer than well-armored bed surfaces are capable of mobilizing and fining the bed surface. The use of gravel significantly finer than the armored surface in gravel augmentation projects could have the desired effect of "unlocking" biologically unproductive armor and of releasing fine, permeability-reducing sediments beneath the coarse surface. The volume of the fine augmentation ultimately dictates how long bed fining and active bed surface transport will persist. The period of elevated transport of the fine tail of the bed surface distribution after passage of the peak may be influenced by pulse volume, but only if significant armor mobilization occurs. In order for strong mobilization and bed surface fining to occur, the size of a fine sediment pulse must not greatly exceed the volume required to cover the bed 1 or 2 D_{50} thick in the reach to be restored because complete local bed coverage negates the local mobilization of bed material, at least until the pulse material on the surface is depleted and the local bed material surface is reexposed. However, when complete coverage does occur, the fine material will translate [*Sklar et al.*, 2009] and lead to downstream mobilization, which may also be a desired outcome of an augmentation.

[54] Smaller fine augmentations are more efficient (i.e., more sediment is mobilized per kilogram of sediment added) at mobilizing bed material than larger pulses. Multiple small pulses are capable of mobilizing marginally more bed material than a single large augmentation of the same volume. In our experiments, mobilization efficiencies increased by ~20% from the first to the second pulse in the multiple pulse experiment, after which the efficiency began to decline. Nevertheless, shorter reaches of channel can be effectively mobilized by multiple small pulses where larger pulses would translate significantly.

[55] Ultimately, a fine sediment pulse is only a useful augmentation technique where mobilization of a coarse surface layer will reveal suitably finer subsurface material. In cases where the depth of subsurface gravel is so limited that a fine augmentation would expose bedrock or in cases where the subsurface material is not within the desired range, an augmentation of the desired subsurface median grain size is more appropriate. For our coarser pulses, changes in the bed surface grain size and bed mobility occur as a result of having the pulse grains on the bed surface. There is some moderate interaction between the bed and coarse pulse material, with some bed material mobilization, but the pulse material is moved instead of the bed material. Periodic augmentations to channels composed of the desired grain size will have a temporary fining effect and could be an effective solution to improving mobility and fining bed surface materials providing that augmentation pulses are added frequently enough to maintain burial of the bed surface.

[56] It is not clear from our experiments what the optimal grain size is for generating the effects we found for our fine and coarse pulses in a gravel augmentation to natural channels. We used pulses that were ~1/5 the median size of the bed surface (~1/4 the size of the subsurface material) and ~2/3 the median size of the bed surface (about the same median size as the subsurface size distribution) (see Figure 2). The fine pulse grain size allowed pulse particles to effectively fill the interstices between larger particles in the surface material, inducing accelerated near bed flow and increased lift and drag on the larger particles. Fine pulses designed to reproduce the behavior we observed should be sized relative to the bed surface so this infilling can occur. Coarse pulses designed to reproduce the behavior we observed should be sized relative to the available flows such that the Shields number calculated using the augmentation grain size is close to the threshold of motion. This will facilitate long-term storage on the surface, burying the

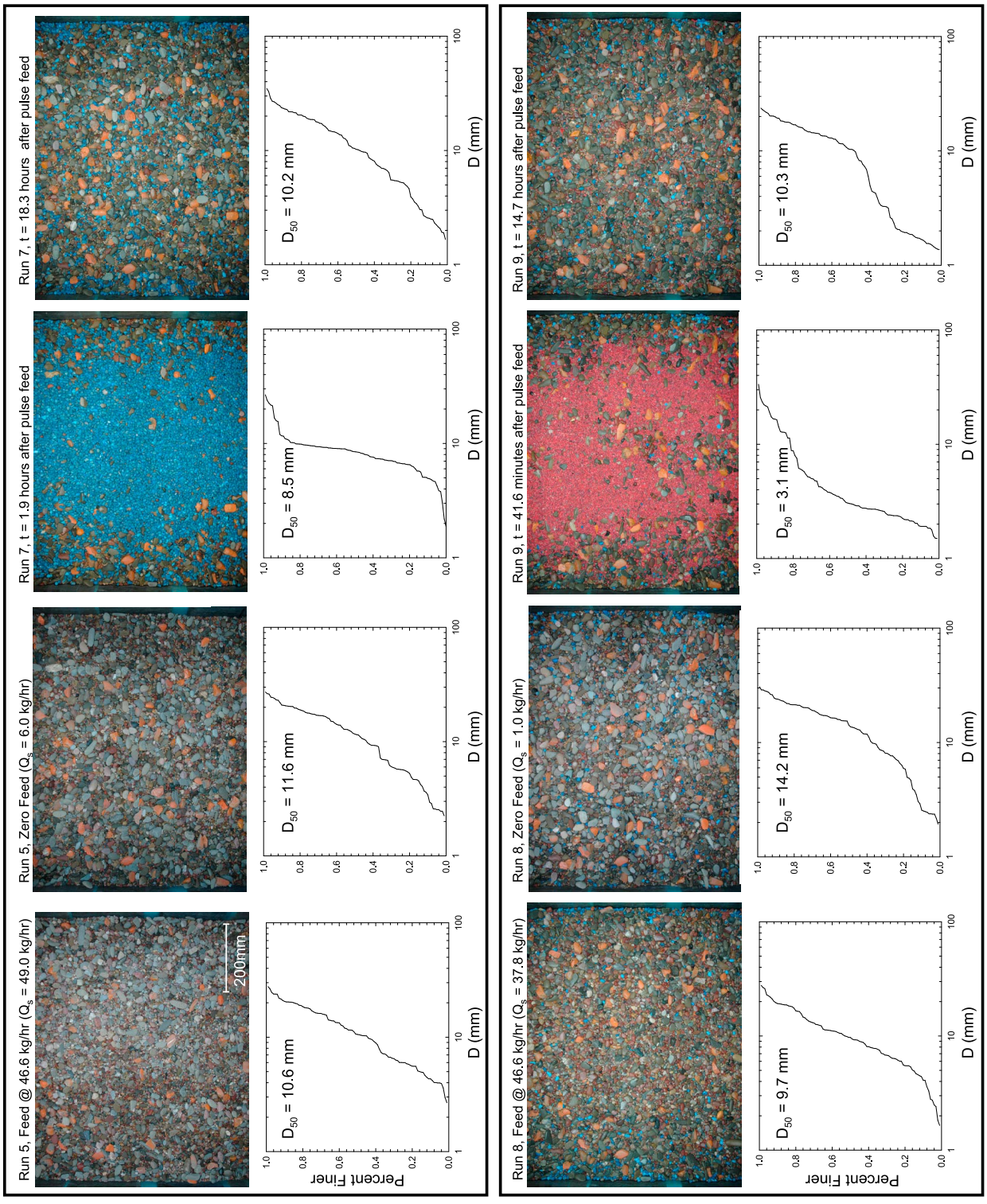

Figure 14. Bed surface images and associated grain size distributions for (top) the large coarse pulse (run 7) and (bottom) the small fine pulse (run 9). Surface grain size distributions were measured from the photos taken 15 m downstream from where the pulses were fed into the channel.

coarse surface layer, but allow periodic flushing and downstream dispersion during mobilizing high flow events.

8. Conclusions

[57] Our results indicate that pulses of sediment in gravel bed rivers that are composed of material finer than the bed surface will interact with the coarse surface layer mobilizing and fining the bed. The effect of fine sediment pulses ~1/5 the median size of the surface is a bimodal bed produced by storage of pulse material at the surface and exposure of finer subsurface material. Coarse pulses ~2/3 the median size of the surface cause less mobilization. There were no long-term changes in the surface armor that occurred as a result of short-lived coarse pulse passages. Fine pulses are more efficient at mobilizing bed material and small transient pulses appear to be more efficient than a single larger pulse. These results suggest that size distribution selection for gravel augmentation should be carefully considered to optimize bed surface mobilization.

[58] **Acknowledgments.** This work was supported by the CALFED Science Program (contact ERP-02D-P55). The instrumentation described herein was designed and constructed by Jim Mullin and Chris Ellis at the National Center for Earth Surface (NCED). Additional support for the equipment, experiments, and analysis was provided by NCED. Technical support for the project was kindly provided by Stuart Foster (UC Berkeley), John Potter (UC Berkeley), and Kurt Yaeger (SFSU). The experimental design benefited from the initial input of the project's scientific advisory panel that included Peter Wilcock (Johns Hopkins University), Gary Parker (University of Illinois), Tom Lisle (U.S. Forest Service), Scott McBain (McBain and Trush, Inc.), Kris Vyverberg (California Department of Fish and Game). Reviews by Peter Wilcock, John Buffington, and an anonymous reviewer greatly improved the manuscript.

References

Bunte, K. (2004), *Gravel mitigation and augmentation below hydroelectric dams: a geomorphological perspective, Stream Systems Technology Center*, 144 pp., USDA Forest Service, Rocky Mountain Research Station, Fort Collins, CO.

Bunte, K., and S. R. Abt (2001), Sampling surface and subsurface particle-size distributions in wadable gravel- and cobble-bed streams for analyses in sediment transport, hydraulics, and stream-bed monitoring: U.S. Department of Agriculture Forest Service Rocky Mountain Research Station General Technical Report RMRS-GTR-74, 428 p.

Church, M. A., D. G. McLean, and J. F. Wolcott (1987), River bed gravels: sampling and analysis, in *Sediment Transport in Gravel Bed Rivers*, edited by C. R. Thorne, J. C. Bathurst, and R. D. Hey, pp. 43–88, John Wiley and Sons, Chichester.

Clayton, J. A., and J. Pitlick (2008), Persistence in the surface texture of a gravel bed river during a large flood, *Earth Surf. Processes Landforms*, *33*, 661–673, doi:10.1002/esp.1567.

Cui, Y., G. Parker, T. E. Lisle, J. Gott, M. E. Hansler-Ball, J. E. Pizzuto, N. E. Allmendinger, and J. M. Reed (2003a), Sediment pulses in mountain rivers: Part I. Experiment, *Water Resour. Res.*, *39*(9), 1239, doi:10.1029/2002WR001803.

Cui, Y., G. Parker, J. E. Pizzuto, and T. E. Lisle (2003b), Sediment pulses in mountain rivers: Part II. Comparison between experiments and numerical predictions, *Water Resour. Res.*, *39*(9), 1240, doi:10.1029/2002WR001805.

Cui, Y., G. Parker, T. E. Lisle, J. E. Pizzuto, and A. M. Dodd (2005), More on the evolution of bed material waves in alluvial rivers, *Earth Surf. Processes Landforms*, *30*, 107–114.

Dietrich, W. E., J. W. Kirchner, H. Ikeda, and F. Iseya (1989), Sediment supply and the development of the coarse surface layer in gravel-bedded rivers, *Nature*, *340*, 215–217.

Gilbert, G. K. (1917), Hydraulic-mining debris in the Sierra Nevada, U.S. Geol. Survey Prof. Paper 105.

Harvey, B., S. McBain, D. Reiser, L. Rempel, L. S. Sklar, and R. Lave (2005), Key uncertainties in gravel augmentation: geomorphological and biological research needs for effective river restoration, CALFED Science Program and Ecosystem Restoration Program Gravel Augmentation Panel report, 99 pp.

Lisle, T. E. (2008), The evolution of sediment waves influenced by varying transport capacity in heterogeneous rivers, in Gravel Bed Rivers VI: From Process Understanding to River Restoration, edited by H. Habersack, H. Piegay, and M. Rinaldi, pp. 443–472, Elsevier, Amsterdam.

Lisle, T. E., F. Iseya, and H. Ikeda (1993), Response of a channel with alternate bars to a decrease in supply of mixed-size bed load: A flume experiment, *Water Resour. Res.*, *29*, 3623–3629.

Lisle, T. E., J. E. Pizzuto, H. Ikeda, F. Iseya, and Y. Kodama (1997), Evolution of a sediment wave in an experimental channel, *Water Resour. Res.*, *33*, 1971–1981.

Lisle, T. E., Y. Cui, G. Parker, J. E. Pizzuto, and A. M. Dodd (2001), The dominance of dispersion in the evolution of bed material waves in gravel bed rivers, *Earth Surf. Processes Landforms*, *26*, 1409–1420.

Kellerhals, R., and D. I. Bray (1971), Sampling procedures for coarse fluvial sediments, *J. Hydraul. Div.-ASCE*, *97*, 1165–1180.

Kondolf, G. M., and M. G. Wolman (1993), The sizes of salmonid spawning gravels, *Water Resour. Res.*, *29*, 2275–2285.

Madej, M. A., and V. Ozaki (1996), Channel response to sediment wave propagation and movement, Redwood Creek, California, USA, *Earth Surf. Processes Landforms*, *21*, 911–927.

Miller, M. C., I. N. McCave, and P. D. Komar (1977), Threshold of sediment motion under unindirectional currents, *Sedimentology*, *41*, 883–903.

Nelson, P. A., J. G. Venditti, W. E. Dietrich, J. W. Kirchner, H. Ikeda, F. Iseya, and L. S. Sklar (2009), Response of bed surface patchiness to reductions in sediment supply, *J. Geophys. Res.*, *114*, F02005, doi:10.1029/2008JF001144.

Parker, G. (2007), Chapter 3: Transport of gravel and sediment mixtures, in *Sedimentation Engineering: Theories, Measurements, Modeling and Practice, ASCE Manual and Reports on Engineering Practice No. 110*, edited by M. H. Garcia, pp. 165–264, American Society of Civil Engineers, Reston, VA.

Parker, G. (2009), 1D Sediment Transport Morphodynamics With Applications to Rivers and Turbidity Currents e-book. (Available at http://cee.uiuc.edu/people/parkerg/morphodynamics_e-book.htm)

Parker, G., and P. C. Klingeman (1982), On why gravel bed streams are paved, *Water Resour. Res.*, *18*, 1409–1423, doi:10.1029/WR018i005p01409.

Roberts, R. G., and M. Church (1986), The sediment budget in severely disturbed watersheds, Queen Charlotte Ranges, British Columbia, *Can. J. Forest Res.*, *16*, 1092–1106.

Sklar, L. S., J. Fadde, J. G. Venditti, P. Nelson, M. A. Wydzga, Y. Cui, and W. E. Dietrich (2009), Translation and dispersion of sediment pulses in flume experiments simulating gravel augmentation below dams, *Water Resour. Res.*, *45*, W08439, doi:10.1029/2008WR007346.

Venditti, J. G., W. E. Dietrich, P. A. Nelson, M. A. Wydzga, J. Fadde, and L. Sklar (2010), Mobilization of coarse surface layers in gravel-bedded rivers by finer gravel bed load, *Water Resour. Res.*, *46*, W07506, doi:10.1029/2009WR008329.

Whiting, P. J., W. E. Dietrich, L. B. Leopold, T. G. Drake, and R. L. Shreve (1988), Bedload sheets in heterogeneous sediment, *Geology*, *16*, 105–108.

Wilcock, P. R., and B. T. DeTemple (2005), Persistence of armor layers in gravel bed streams, *Geophys. Res. Lett.*, *32*, L08402, doi:10.1029/2004GL021772.

Williams, G. P. (1970), Flume width and water depth effects in sediment transport experiments, USGS Professional Paper, 37, 562-H.

Wolman, M. G. (1967), A cycle of sedimentation and erosion in urban river channels, *Geogr. Ann.*, *49*, 385–395.

Yalin, M. S., and E. Karahan (1979), Inception of sediment transport, *J. Hydraul. Div.-ASCE*, *105*, 1433–1443.

W. E. Dietrich and P. A. Nelson, Department of Earth and Planetary Science, University of California, Berkeley, CA 94720, USA.

J. Fadde and L. Sklar, Department of Geosciences, San Francisco State University, San Francisco, CA 94132, USA.

J. G. Venditti, Department of Geography, Simon Fraser University, Burnaby, BC V5A 1S6, Canada. (jgvenditti@yahoo.ca)

M. A. Wydzga, Department of Earth Science, University of California-Santa Barbara, Santa Barbara, CA 93106, USA.